science, engineering and health studies

Research Article

Science, Engineering and Health Studies
https://lio1.tci-thaijo.org/index.php/sehs
ISSN (Online): 2630-0087

Comparison of stress distribution on articular disc between the Hunsuck/Epker and NM-Low Z plasty technique for mandibular setback procedure

Chutiwat Sakyanun[1], Narissaporn Chaiprakit[1], Samroeng Inglam[2], and Siripatra Patchanee[3]*

[1] Division of Oral and Maxillofacial Surgery, Faculty of Dentistry, Thammasat University, Pathum Thani 12120, Thailand
[2] Division of Oral Diagnostic Science and Maxillofacial Surgery, Faculty of Dentistry, Thammasat University, Pathum Thani 12120, Thailand
[3] Division of Orthodontics, Faculty of Dentistry, Thammasat University, Pathum Thani 12120, Thailand

***Corresponding author**: Siripatra Patchanee
siripatra.p@hotmail.com*

***Received**: 2 August 2024*
***Revised**: 24 April 2024*
***Accepted**: 19 June 2024*
***Published**: 19 December 2024*

***Citation**: Sakyanun, C., Chaiprakit, N., Inglam, S., and Patchanee, S. (2024). Comparison of stress distribution on articular disc between the Hunsuck/Epker and NM-Low Z Plasty technique for mandibular setback procedure. Science, Engineering and Health Studies, 18, 24050020.*

ABSTRACT

Novel modification of Low Z plasty (NM-Low Z) technique is a bilateral sagittal split osteotomy (BSSO) technique in which the incision line is designed to create more inferior support at the proximal segment compared to the Hunsuck/Epker (HE) modification. This study aimed to evaluate and compare the stress distribution patterns at the articular disc of the temporomandibular joint (TMJ) using the NM-Low Z technique and HE modification in mandibular prognathism models. Finite element models of the mandible including the TMJ from a CT scan of a patient with skeletal class III deformity that required mandibular setback surgery, were segmented using the NM-Low Z and HE modification techniques. The mandible was moved 7 mm posteriorly and fixed with 2.0 mm miniplates and screws. The material properties of the articular discs were simulated as homogenous, isotropic, and linear elastic materials. Finite element analysis was used to evaluate the equivalent von Mises stress on the articular disc of the TMJ. Various muscular and biting forces were applied to simulate 1, 3, and 12 months postoperatively in both models. The maximum von Mises stresses of the articular disc in the NM-Low Z model were 60.64, 36.43, and 76.38 MPa, while those of the HE modification model were 73.40, 29.94, and 82.51 MPa at 1, 3, and 12 months, respectively. Both techniques resulted in normal stress distribution patterns on the articular disc surface. In conclusion, the NM-Low Z technique is an option for BSSO in terms of providing a lower maximum von Mises stress at the articular disc than the HE modification technique, while also providing a normal stress distribution pattern similar to the HE modification technique.

Keywords: NM Low Z plasty; orthognathic surgery; temporomandibular joint; bilateral sagittal split osteotomy; skeletal III; finite element analysis

1. INTRODUCTION

Bilateral sagittal split osteotomy (BSSO) is the most common orthognathic surgery performed to correct mandibular prognathism. To correct mandibular prognathism, the BSSO procedure aims to split the mandible into two segments: the proximal (composed of the ramus and condyle of the mandible) and the distal segment (composed of the alveolar bone and teeth). The distal segment is then placed backward, called the mandibular setback, in the desired position. Several modifications of BSSO have been established to improve operator convenience, decrease morbidity, and maximize procedural stability (Böckmann et al., 2014). The Hunsuck/Epker (HE) modification has gained popularity due to decreased damages to the inferior alveolar nerve and prevention from potentially bad splits (Yang et al., 2007). This HE technique requires detaching the temporalis muscle to the level of the sigmoid notch to ensure that the medial horizontal osteotomy incision has enough access (Epker, 1977). However, the HE modification has been reported with incidences of postoperative complications including skeletal relapse, condylar resorption, and temporomandibular joint disorder (TMD) (Mitsukawa et al., 2013).

The novel modification of Low Z plasty technique has several advantages over BSSO modifications. Using this technique, bony interference at the inner surface of the proximal segment must be removed. Therefore, this technique can further extend movement of the distal segment of the mandible. This lack of interference can prevent loading torque at the mandibular condyle of the proximal segment, thereby providing good skeletal stability. According to finite element analysis by Dumrongwanich et al. (2022), the NM-Low Z technique had lower maximum EQV stress on miniplate and bone than the HE modification technique. Another study reported on clinical evaluation by cephalometric analysis of skeletal changes after mandibular setback surgery by the NM-Low Z technique. The mandible had a tendency to relapse in a forward and upward direction (Imampai et al., 2022).

In patients with mandibular prognathism who underwent orthognathic surgical correction, the signs and symptoms of TMD, such as pain in the TMJs and/or muscles of mastication, were observed. TMJ sounds during function and limitation in the range of mandibular motion were found in approximately 16.8–24% of operative patients (Togashi et al., 2013). The signs and symptoms associated with TMJs have been reported to improve one year after orthognathic surgery. However, if the TMJ load increases substantially after surgery, TMD symptoms may emerge (Kobayashi et al., 1999). According to biomechanical research, postoperative complications have been linked with changing in stress distribution around the osteotomy area and the TMJ postoperatively. There were more compressive stresses at the articular disc in patients with mandibular prognathism than that in normal patients, especially in those with mandibular prognathism and TMD reported (Ma et al., 2020). Moreover, the ability of BSSO modification to improve stress distribution on the TMJ has been established (Liu et al., 2018; Ma et al., 2020).

The majority of studies have evaluated the changes in the TMJ and articular disc morphology and position after BSSO using magnetic resonance imaging (MRI) and cone-beam computed tomography (CBCT) (Kang et al., 2020; Kim et al., 2009; Takahara et al., 2017; Ueki et al., 2002, 2012). Few studies have examined the biomechanical changes in stress distribution in TMJs following BSSO. Although different positions of the BSSO surgical osteotomy between the NM-Low Z and HE modification techniques have been studied, there are no studies comparing the stress distribution at the TMJ disc between the two techniques. Accordingly, it is important to understand the biomechanical effects and stress distribution on the TMJ disc to analyze the effects of the NM-Low Z technique on the mandibular setback procedure. The aim of this study was to evaluate and compare the effects of the NM-Low Z and HE modification techniques on the stress distribution pattern at the articular disc of the TMJs.

2. MATERIALS AND METHODS

This study involved the development of a finite element (FE) model of the TMJ using simulated mandibular models with two osteotomy techniques in three postoperative stages. Different magnitudes of muscle forces and biting loads were applied at each stage. The biting loads and muscle forces used in this study were applied at the right canine, premolar, first molar, and second molar.

The inclusion criteria to select a patient CT file was a patient with skeletal class III deformity that required mandibular setback surgery, facial symmetry, without history of TMJ-related therapies.

2.1 Geometry

The structure of the model was created using whole-skull medical CT images with a slice thickness of 0.625 (Spectral CT 7500, Philips, USA) of a patient with a prognathic mandible and asymptomatic TMJs on both sides without a medical history of craniofacial syndrome or previous maxillofacial trauma. The cortical and cancellous bone geometries were digitally scanned and located using different Hounsfield unit (HU) threshold values. The HU unit value ranged from +300 to +400 in cancellous bone, +1800 to +1900 in cortical bone, and above +2200 in enamel (Patrick et al., 2017). The 3D models of the mandible and glenoid fossa of temporal bones were created from the Digital Imaging and Communications in Medicine (DICOM) file format in image processing software (3D Slicer software, slicer.org) (Fedorov et al., 2012) (Figure 1).

In this study, the authors considered the cartilage to be a part of the mandible and temporal bone in our models and observed the stress distribution experienced at the articular disc elements. Thus, the articular cartilage was disregarded. The articular disc model was created using the space between the glenoid fossa and mandibular condylar head with 3D parametric computer-aided design (CAD) software (VISI, Hexagon AB, Sweden). The final 3D geometric models were exported from VISI as standard tessellation language (STL) files (Figure 2).

Simulations of osteotomies using the HE modification and NM-low Z techniques were generated in FEM as the operative plan (mandibular setback 7 mm) (Figure 3).

In the HE modification technique, the horizontal osteotomy was placed just superior and posterior to the lingula of the mandible, and the sagittal osteotomy was continued with a higher oblique osteotomy line along the external oblique ridge of the mandible. A vertical osteotomy was then performed from the mesial aspect of the second molar to the lower border of the mandible (Epker, 1977).

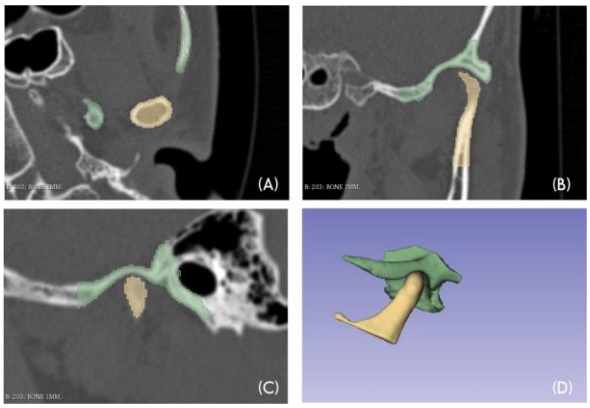

Figure 1. 3D models of the mandibular condyle and glenoid fossa of the temporal bone were developed in the 3D slicer program using DICOM file format: (A) axial view, (B) coronal view, (C) sagittal view, and (D) 3D model of temporomandibular joint

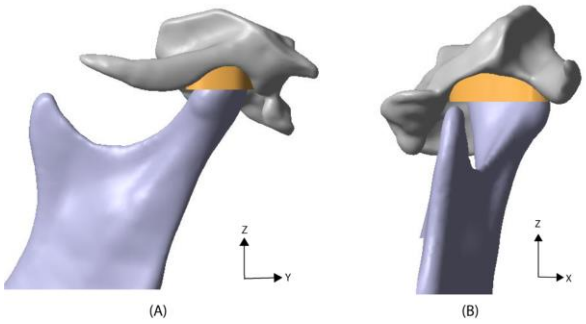

Figure 2. 3D geometric model of the temporomandibular joint composed of glenoid fossa of temporal bone, articular disc, and condyle of mandible: (A) lateral view and (B) frontal view

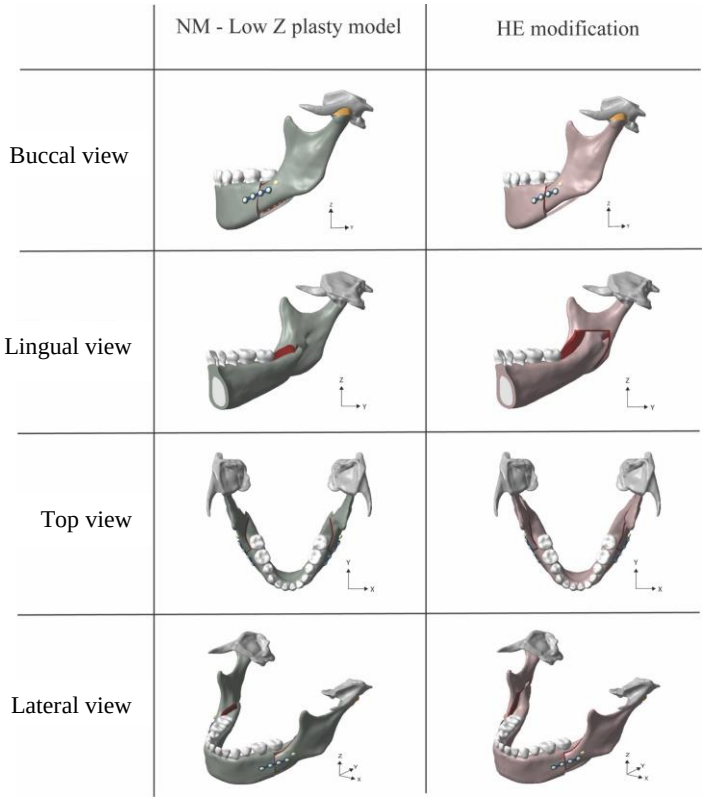

Figure 3. 3D models of novel modification of low Z plasty technique and the Hunsuck/Epker modification technique containing TMJ structure

In the NM-Low Z technique, a horizontal osteotomy was performed at the most superior point of the retromolar triangle. Sagittal osteotomy was performed laterally along the external oblique ridge to the buccal alveolar bone. A vertical osteotomy was performed inferiorly through the inferior border of the mandible in the area of the second mandibular molar (Chaiprakit et al., 2021).

The osteotomy line was set to a thickness of 1 mm and the model was separated into proximal and distal segments of the mandible on both sides after completing the osteotomy. The distal segment was set backwards 7 mm according to the surgical plan. Finally, bilateral rigid fixation was performed using miniplates and screws. The titanium locking miniplate model was simulated as 1.0-mm thickness with four holes. Four titanium monocortical screws with a 2.0-mm diameter and 6.0-mm length were used. Miniplates and four monocortical screws were used to secure the overlapping portions of the proximal and distal segments that were placed along Champy's line. The authors assumed that there was no slippage at the interface between the plate hole and screw or between the screws and the bone. In addition, bicortical titanium screws were simulated with 2.0 mm in diameter and 18.0 mm in length and placed bilaterally in the proximal segment area in the retromolar regions (Dumrongwanich et al., 2022).

2.2 Material properties

According to a previous study, the biomechanical properties of the cortical bone, cancellous bone, titanium, dentition, and articular disc (Pinheiro et al., 2021) were assumed to be homogeneous, isotropic, and linearly elastic. The material properties are listed in Table 1. Clinically one month after the surgery, the cancellous bone between the proximal and distal segments initially healed. Therefore, the material characteristics of the cancellous bone was considered as new bone tissue (Li et al., 2020). Three months after the surgery, the cortical bone between the two segments had almost healed, the elastic modulus of the new cortical bone was 10,000 Pa (Liu et al., 2018). Twelve months after the surgery, the cortical bone of the mandible had completely healed. The material property was considered cortical bone (Li et al., 2020).

Table 1. Material properties

	Young's modulus (MPa)	Poisson's ratio
Cortical bone (Li et al., 2020)	13,700	0.3
Cancellous bone (Li et al., 2020)	7,930	0.3
Articular disc (Pinheiro et al., 2021)	16	0.4
Tooth (Pinheiro et al., 2021)	20,000	0.3
New cortical bone, three months after surgery (Liu et al., 2018)	10,000	0.3
Titanium (Pinheiro et al., 2021)	113,800	0.34

2.3 Loading and boundary conditions

The two models were fitted with the force vectors of the bilateral masticatory muscles corresponding to the static clenching task in the right canine (F1), premolar (F2), first molar (F3), and second molar (F4). Six muscles were considered in this study: the superficial masseter muscle (SM), deep masseter muscle (DM), anterior temporalis muscle (AT), middle temporalis muscle (MT), posterior temporalis muscle (PT), and medial pterygoid muscle (MP)(Huang et al., 2015). The magnitude and direction of the six muscular forces are listed in Table 2. Constrained regions were indicated in the temporal bone on both sides (Figure 4).

Postsurgical bite force was varied at each time point according to previous literature reported in patients with mandibular prognathism (Choi et al., 2014). Both surgical models had applied total bite forces of 97.6 N, 206.9 N, and 397 N postoperatively at 1, 3, and 12 months, respectively. The postsurgical bite force was applied to analyze the influence of BSSO on the TMJs when biting on the right side. The average loads of applied forces (F1, F2, F3, and F4) were of 24.4 N, 51.7 N, and 99.3 N in postoperatively at 1, 3, and 12 months, respectively (Choi et al., 2014).

2.4 Contact conditions

The models used in this analysis consisted of several parts. Therefore, contact conditions were established between the individual parts of the models. By determining the bone components, the monocortical screws and temporomandibular joints could be locked. No relative translative was assigned between the bony segments, bone-articular disc, or bone-tooth, disabling them from moving away from each other. Frictionless relative displacement with a friction coefficient of 0.3 was assigned to miniplates and bones as well as bicortical screws and bones (Dumrongwanich et al., 2022).

2.5 Element generation and convergence test

The 3D solid models in this study were generated with four-noded tetrahedral elements using automatic mesh generation software (MSC Patran; MSC Software, Inc., USA) based on a 3D CAD model of the mandible, temporal bone, and articular disc. The element size of the articular disc was finer than that of the other regions. Based on the convergence test results, the appropriate number of elements for each FE model was calculated. The HE modification technique established a mesh model with 90,851 nodes (424,245 elements), and the NM-Low Z technique had 94,467 nodes (382,243 elements).

The postoperative models were simulated based on the features of the mandibular osteotomy technique. Six models were created using two different surgical techniques at three time points. For each model, the maximum Von Mises stress and stress distribution at the articular disc were observed.

3. RESULTS

The results illustrated the maximum von Mises stress and stress distributions at the articular disc after mandibular setback surgery in a patient with mandibular prognathism during the static clenching task at right canine, premolar, first molar, and second molar at 1, 3, and 12 months as shown in Table 3.

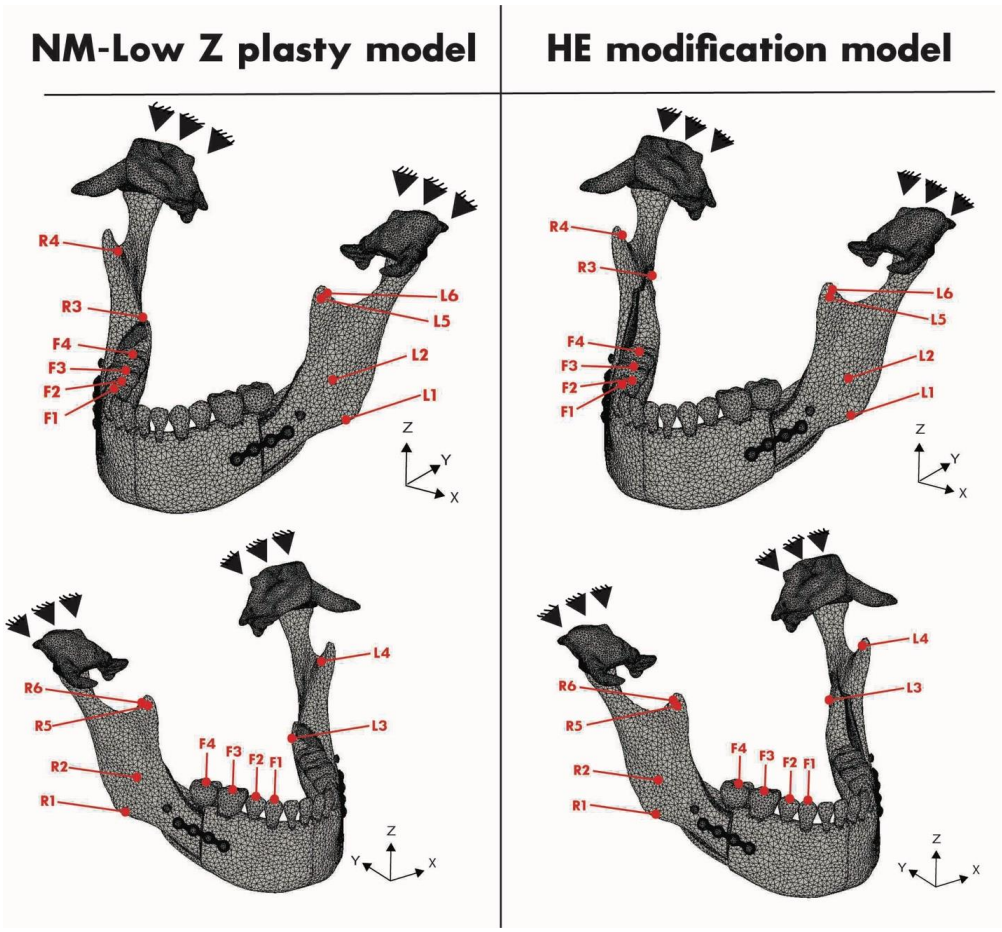

Figure 4. All load points on the models including muscular force (R; right muscular force, L; left muscular force), biting force (F), and constraints area at temporal bones on both sides applied in finite element simulation

Table 2. Muscular forces and direction of the biting force on the right side (Choi et al., 2014)

Point	Force	Direction and magnitude(N)								
		1-month postoperative			3-month postoperative			12-month postoperative		
		X	Y	Z	X	Y	Z	X	Y	Z
R1	Right SM	-7.1	-14.4	30.3	-7.1	-14.4	30.3	-7.1	-14.4	30.3
R2	Right DM	-16.0	10.5	22.3	-16.0	10.5	22.3	-16.0	10.5	22.3
R3	Right MP	6.0	-4.6	9.7	6.0	-4.6	9.7	6.0	-4.6	9.7
R4	Right AT	-15.5	-4.6	103.0	-15.5	-4.6	103.0	-15.5	-4.6	103.0
R5	Right MT	-13.6	30.6	51.2	-13.6	30.6	51.2	-13.6	30.6	51.2
R6	Right PT	9.8	40.1	22.2	9.8	40.1	22.2	9.8	40.1	22.2
L1	Left SM	10.6	-21.5	45.4	10.6	-21.5	45.4	10.6	-21.5	45.4
L2	Left DM	11.6	7.6	16.1	11.6	7.6	16.1	11.6	7.6	16.1
L3	Left MP	-64.6	-49.6	105.1	-64.6	-49.6	105.1	-64.6	-49.6	105.1
L4	Left AT	1.7	-0.5	10.9	1.7	-0.5	10.9	1.7	-0.5	10.9
L5	Left MT	1.3	2.9	4.8	1.3	2.9	4.8	1.3	2.9	4.8
L6	Left PT	0.9	3.9	2.2	0.9	3.9	2.2	0.9	3.9	2.2
F1	Right canine	0	0	-24.4	0	0	-51.7	0	0	-99.3
F2	Right premolar	0	0	-24.4	0	0	-51.7	0	0	-99.3
F3	Right first molar	0	0	-24.4	0	0	-51.7	0	0	-99.3
F4	Right second molar	0	0	-24.4	0	0	-51.7	0	0	-99.3

Note: SM = superficial masseter; DM = deep masseter; MP = medial pterygoid; AT = anterior temporalis; MT = middle temporalis; and PT = posterior temporalis

Table 3. Summarization for maximum von Mises stress and area at articular disc during biting force at 1, 3, and 12 months

	HE modification model				**NM-Low Z model**			
	Max. von Mises stress (MPa)		**Area**		**Max. von Mises stress (MPa)**		**Area**	
	Right	Left	Right	Left	Right	Left	Right	Left
1 month	73.40	72.11	Lateral part, Intermediate zone	Lateral part, Intermediate zone	52.60	60.64	Posterior part, Intermediate zone	Posterior part, Intermediate zone
3 months	29.94	28.36	Lateral part, Intermediate zone	Lateral part, Intermediate zone	36.40	36.43	Posterior part, Intermediate zone	Posterior part, Intermediate zone
12 months	82.51	69.88	Posterior part, Lateral part	Posterior part, Lateral part	76.38	51.92	Posterior part, Lateral part	Posterior part, Lateral part

One month after surgery, the distribution of the von Mises stress at the articular disc in the NM-Low Z technique had a more uniform force distribution in the area than the HE modification technique, and the maximum von Mises stress of the HE modification technique was 73.4 MPa on the right side and 72.1 MPa on the left side. In contrast, the NM-Low Z technique had a maximum von Mises stress of 52.6 MPa on the right side and 60.64 MPa on the left side. The maximum von Mises stress area of the HE modification technique was in the intermediate and lateral parts of the band, whereas that of the NM-Low Z technique was distributed throughout the intermediate and posterior parts of the band.

At three months postoperative, the maximum von Mises stress for the HE modification and NM-Low Z techniques was reduced, and the HE modification technique was 29.94 MPa on the right side and 28.36 MPa on the left side. The NM-Low Z technique was 36.4 MPa on the right side and 36.43 on the left. The maximum von Mises stress locations for both methods were the load points. The maximum von Mises stress of the HE modification technique was found in the intermediate zone and lateral part of the band on both sides of the articular disc, whereas the maximum von Mises stress of the NM-Low Z technique was found in the intermediate and posterior part of the band on both sides.

At twelve months postoperative, patients had developed greater bite force than that before surgery (Choi et al., 2014). The maximum von Mises stress at the articular disc had increased. The HE modification technique values were 82.51 MPa on the right side and 69.88 MPa on the left side. The NM-Low Z technique was 76.38 MPa on the right side and 51.92 MPa on the left side. Both techniques presented the maximum von Mises stresses at the lateral and posterior parts of the band. The stress distribution pattern of the articular disc of the TMJ is shown in Figure 5 (inferior surface) and Figure 6 (superior surface).

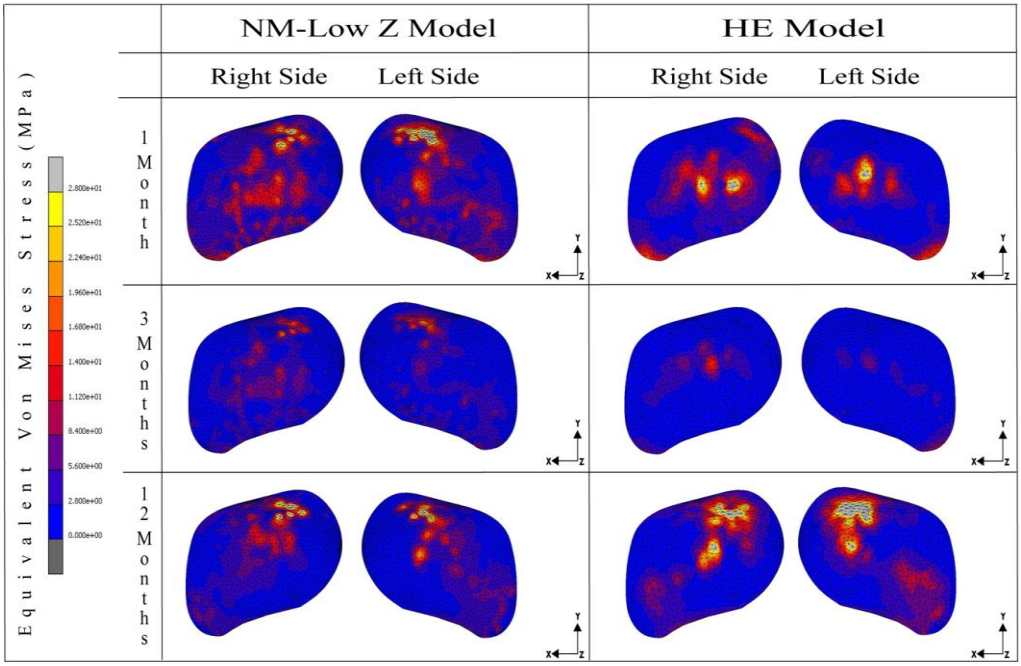

Figure 5. The von Mises stress distributions of the articular disc between the NM-Low Z and HE modification model, 1, 3, and 12 months postoperative: inferior surface

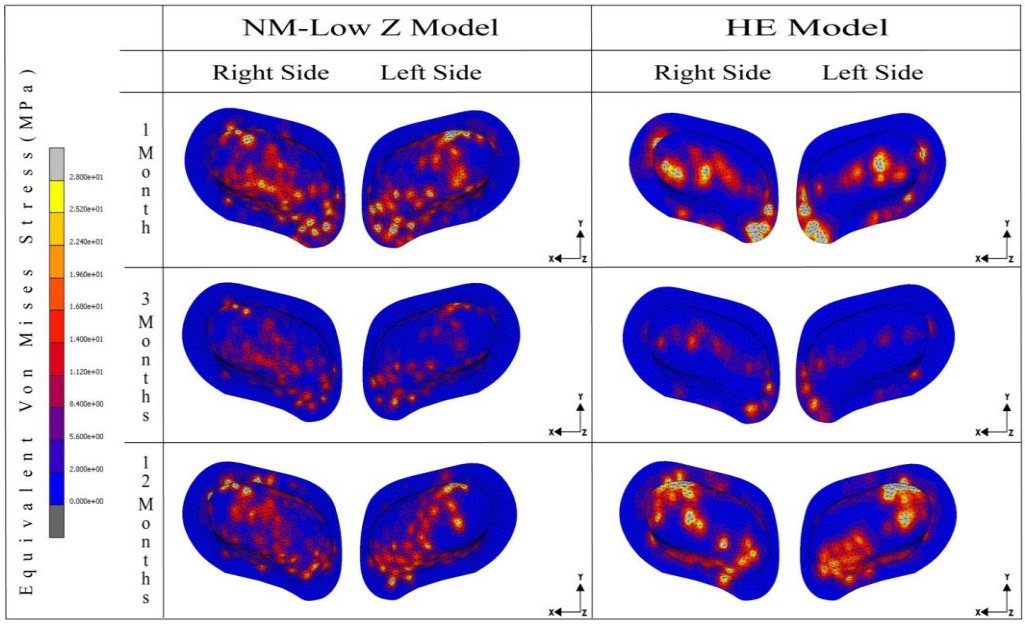

Figure 6. The von Mises stress distributions of articular disc between the NM-Low Z and HE modification model, 1, 3, and 12 months postoperative: superior surface

4. DISCUSSION

At different postoperative times (1, 3, and 12 months), the material properties at the osteotomy site and the biting force varied. Previous studies have shown that bite forces in healthy people can decline by 50% or more during the postoperative period and then progressively return to normal after 3 months to 2 years (Choi et al., 2014; Harada et al., 2003). Moreover, the FEM can help in predicting the impact of different surgical techniques on the articular disc by applying different muscular forces and biting loads.

The stress distribution in the TMJ of a patient with mandibular prognathism was higher than that in a normal TMJ. Moreover, long-term symmetric occlusion can cause the intermediate zone of the articular disc to perforate or become thin (Ma et al., 2020). Kobayashi et al. (1999) reported no statistically significant correlation between TMJ symptoms and disc displacement. Patients with disc displacement did not necessarily have TMJ signs and symptoms, while patients with symptoms did not always have disc displacement. However, the contact area and contact stress between the articular disc and bones after BSSO were lower than those before surgery (Liu et al., 2018). The NM-Low Z technique was introduced by Chaiprakit et al. (2021). This mandibular osteotomy technique was modified from Low Z plasty (Prasan's modification) and was used in our center (Tangarturonrasme and Sununliganon, 2016). The horizontal osteotomy incision line of the NM-Low Z technique is located in the retromolar area, which is much lower than that of the HE modification technique.

In our previous study (Dumrongwanich et al., 2022), the NM-Low Z technique was shown to induce less bone stress around the screws than the HE modification technique. The NM-Low Z technique provides inferior support between the proximal and distal segments of the mandibular setback. To compare the maximum von Mises stress between the right and left sides of the articular disc after surgery, the biting force on the right side was used as a clenching task.

In this study, 1 month after surgery, the maximum von Mises stress at the articular disc of the HE modification technique was higher than that of the NM-Low Z technique on both right and left sides. The maximum von Mises stresses of both techniques were located commonly in the intermediate zone, which is consistent with the study by Liu et al. (2018). The shape of the mandible after mandibular setback along with the loads changed after orthognathic surgery. One month after BSSO, functional training should use reasonably low biting forces to prevent postoperative TMDs. Moreover, while using the HE modification technique for mandibular setbacks, the surgeon must identify the lingula of the mandible by detaching the temporalis muscle tendon, thus leading to muscle injury and trismus. This may explain why the NM-Low Z technique causes less stress to the articular disc than the HE modification technique.

Three months after surgery, the maximum von Mises stress was located in the intermediate and lateral part of the band in the HE modification technique and in the intermediate and posterior part of the band in the NM-Low Z technique. The stress distribution patterns of the articular disc tended to be normal in both techniques at 12 months after surgery. However, a more uniform force distribution pattern was observed in the NM-Low Z technique. The maximum von Mises stress of the NM-Low Z technique was lower than that of the HE modification technique on both sides. This is in line with previous studies (Dumrongwanich et al., 2022; Puricelli et al., 2007). Lower levels of stress and displacements were produced as a result of the shorter lever arm size applied to the mandible in the NM-Low Z technique, which results in higher stability of the bone segments. The maximum von

Mises stresses were located at the lateral and posterior parts of the band in both techniques, which are related to the normal stress distribution pattern of the normal TMJ (Lai et al., 2020; Liu et al., 2018).

Therefore, the HE modification and the NM-Low Z techniques can improve the stress distribution on the articular disc in patients with mandibular prognathism. Moreover, the NM-Low Z technique provided lower stress distribution at the articular disc, which could prevent the risk of disc thinning and perforation (Lai et al., 2020).

Several limitations of the current study must be mentioned. First, because of various biological factors in humans, the biomechanical characteristics of articular discs tend to change (Kijak et al., 2020). For stress analysis on the articular disc that composes of the fibrocartilage, the material properties should be represented using a hyperelastic material and should exhibit anisotropy and inhomogeneity. According to previous studies (Liu et al., 2018; Ma et al., 2020; Pinheiro et al., 2021; Shu et al., 2019), the material property of the articular disc was assumed to be homogenous, isotropic, and linearly elastic for simplification. Secondly, the articular disc models were constructed from CT images in accordance with anatomical space between glenoid fossa of the temporal bone and condylar head of the mandible. Results from the loading measurements were presented by loading points during biting force instead of loading at the entire region of contact. In FE analysis, bone frequently models as isotropic, but it is the heterogeneous and anisotropic nature of bone tissue. In our study, bone was modeled as homogenous, isotropic, and linearly elastic. Another limitation of this study is that, the geometric representative of the articular disc in our FE model was simplified to facilitate computational analysis, potentially limiting the accuracy and realism of the simulation. This study focused on the mandibular setback procedure. The different surgical techniques for BSSO could produce different areas of stress distribution and magnitude of stress on the TMJ. Thus, stress analysis at the TMJ would be a further benefit on studying mandibular advancement and rotation.

5. CONCLUSION

This study used FE analysis to study the maximum von Mises stress and stress distribution pattern at the articular disc of TMJs. In patients with mandibular prognathism, NM-low Z technique could provide less stress at the articular disc of TMJs in mandibular setback compared to the HE modification technique.

ACKNOWLEDGMENT

We extend our gratitude to the Faculty of Engineering, Kasetsart University, Sriracha Campus for providing the facilities used in this study. There are no conflicts of interest regarding this publication. This study was approved by the Ethical Review Sub-Committee Board for Human Research Involving Sciences No.3 at Thammasat University, Thailand in accordance with the Declaration of Helsinki, the Belmont report, CIMOS guidelines, and international practice (ICH-GCP); Project No. 005/2565.

REFERENCES

Böckmann, R., Meyns, J., Dik, E., and Kessler, P. (2014). The modifications of the sagittal ramus split osteotomy: A literature review. *Plastic and Reconstructive Surgery Global Open*, 2(12), e271.

Chaiprakit, N., Oupadissakoon, C., Klaisiri, A., and Patchanee, S. (2021). A surgeon-friendly BSSO by the novel modification of low Z plasty: Approach focus and case report: A case report. *Journal of International Dental and Medical Research*, 14(2), 768–772.

Choi, Y. J., Lim, H., Chung, C. J., Park, K. H., and Kim, K. H. (2014). Two-year follow-up of changes in bite force and occlusal contact area after intraoral vertical ramus osteotomy with and without Le Fort I osteotomy. *International Journal of Oral and Maxillofacial Surgery*, 43(6), 742–747.

Dumrongwanich, O., Chantarapanich, N., Patchanee, S., Inglam, S., and Chaiprakit, N. (2022). Finite element analysis between Hunsuck/Epker and novel modification of low Z plasty technique of mandibular sagittal split osteotomy. *Proceedings of the Institution of Mechanical Engineers, Part H: Journal of Engineering in Medicine*, 236(5), 646–655.

Epker, B. N. (1977). Modifications in the sagittal osteotomy of the mandible. *Journal of Oral Surgery (American Dental Association: 1965)*, 35(2), 157–159.

Fedorov, A., Beichel, R., Kalpathy-Cramer, J., Finet, J., Fillion-Robin, J.-C., Pujol, S., Bauer, C., Jennings, D., Fennessy, F., Sonka, M., Buatti, J., Aylward, S., Miller, J. V., Pieper, S., and Kikinis, R. (2012). 3D slicer as an image computing platform for the quantitative imaging network. *Magnetic Resonance Imaging*, 30(9), 1323–1341.

Harada, K., Kikuchi, T., Morishima, S., Sato, M., Ohkura, K., and Omura, K. (2003). Changes in bite force and dentoskeletal morphology in prognathic patients after orthognathic surgery. *Oral Surgery, Oral Medicine, Oral Pathology, Oral Radiology, and Endodontology*, 95(6), 649–654.

Huang, H.-L., Su, K.-C., Fuh, L.-J., Chen, M. Y. C., Wu, J., Tsai, M.-T., and Hsu, J.-T. (2015). Biomechanical analysis of a temporomandibular joint condylar prosthesis during various clenching tasks. *Journal of Cranio-Maxillofacial Surgery*, 43(7), 1194–1201.

Imampai, S., Patchanee, S., Klaisiri, A., and Chaiprakit, N. (2022). Evaluation of skeletal changes after mandibular setback surgery using the NM-Low Z plasty technique in skeletal class III patients. *European Journal of Dentistry*, 17(2), 381–386.

Kang, H.-S., Han, J. J., Jung, S., Kook, M.-S., Park, H.-J., and Oh, H.-K. (2020). Comparison of postoperative condylar changes after unilateral sagittal split ramus osteotomy and bilateral sagittal split ramus osteotomy using 3-dimensional analysis. *Oral Surgery, Oral Medicine, Oral Pathology and Oral Radiology*, 130(5), 505–514.

Kijak, E., Margielewicz, J., and Pihut, M. (2020). Identification of biomechanical properties of temporomandibular discs. *Pain Research and Management*, 2020, 6032832.

Kim, Y.-K., Yun, P.-Y., Ahn, J.-Y., Kim, J.-W., and Kim, S.-G. (2009). Changes in the temporomandibular joint disc position after orthognathic surgery. *Oral Surgery, Oral Medicine, Oral Pathology, Oral Radiology, and Endodontology*, 108(1), 15–21.

Kobayashi, T., Honma, K., Izumi, K., Hayashi, T., Shingaki, S., and Nakajima, T. (1999). Temporomandibular joint symptoms and disc displacement in patients with mandibular prognathism. *British Journal of Oral and Maxillofacial Surgery*, 37(6), 455–458.

Lai, L., Huang, C., Zhou, F., Xia, F., and Xiong, G. (2020). Finite elements analysis of the temporomandibular joint disc in patients with intra-articular disorders. *BMC Oral Health*, 20, 93.

Li, H., Zhou, N., Huang, X., Zhang, T., He, S., and Guo, P. (2020). Biomechanical effect of asymmetric mandibular prognathism treated with BSSRO and USSRO on temporomandibular joints: A three-dimensional finite element analysis. *British Journal of Oral and Maxillofacial Surgery*, 58(9), 1103–1109.

Liu, Z., Shu, J., Zhang, Y., and Fan, Y. (2018). The biomechanical effects of sagittal split ramus osteotomy on temporomandibular joint. *Computer Methods in Biomechanics and Biomedical Engineering*, 21(11), 617–624.

Ma, H., Shu, J., Wang, Q., Teng, H., and Liu, Z. (2020). Effect of sagittal split ramus osteotomy on stress distribution of temporomandibular joints in patients with mandibular prognathism under symmetric occlusions. *Computer Methods in Biomechanics and Biomedical Engineering*, 23(16), 1297–1305.

Mitsukawa, N., Morishita, T., Saiga, A., Kubota, Y., Omori, N., Akita, S., and Satoh, K. (2013). Dislocation of temporomandibular joint: Complication of sagittal split ramus osteotomy. *Journal of Craniofacial Surgery*, 24(5), 1674–1675.

Patrick, S., Birur, N. P., Gurushanth, K., Raghavan, A. S., and Gurudath, S. (2017). Comparison of gray values of cone-beam computed tomography with Hounsfield units of multislice computed tomography: An *in vitro* study. *Indian Journal of Dental Research*, 28(1), 66–70.

Pinheiro, M., Willaert, R., Khan, A., Krairi, A., and Van Paepegem, W. (2021). Biomechanical evaluation of the human mandible after temporomandibular joint replacement under different biting conditions. *Scientific Reports*, 11(1), 14034.

Puricelli, E., Fonseca, J. S. O., de Paris, M. F., and Sant'Anna, H. (2007). Applied mechanics of the Puricelli osteotomy: A linear elastic analysis with the finite element method. *Head & Face Medicine*, 3, 38.

Shu, J., Zhang, Y., and Liu, Z. (2019). Biomechanical comparison of temporomandibular joints after orthognathic surgery before and after design optimization. *Medical Engineering & Physics*, 68, 11–16.

Takahara, N., Kabasawa, Y., Sato, M., Tetsumura, A., Kurabayashi, T., and Omura, K. (2017). MRI changes in the temporomandibular joint following mandibular setback surgery using sagittal split ramus osteotomy with rigid fixation. *CRANIO*, 35(1), 38–45.

Tangarturonrasme, P., and Sununliganon, L. (2016). Modified bilateral sagittal split osteotomy for correction of severe anterior open bite: Technical note and case report. *Chulalongkorn Medical Journal*, 60(1), 45–54.

Togashi, M., Kobayashi, T., Hasebe, D., Funayama, A., Mikami, T., Saito, I., Hayashi, T., and Saito, C. (2013). Effects of surgical orthodontic treatment for dentofacial deformities on signs and symptoms of temporomandibular joint. *Journal of Oral and Maxillofacial Surgery, Medicine, and Pathology*, 25(1), 18–23.

Ueki, K., Marukawa, K., Nakagawa, K., and Yamamoto, E. (2002). Condylar and temporomandibular joint disc positions after mandibular osteotomy for prognathism. *Journal of Oral and Maxillofacial Surgery*, 60(12), 1424–1432.

Ueki, K., Moroi, A., Sotobori, M., Ishihara, Y., Marukawa, K., Yoshizawa, K., Kato, K., and Kawashiri, S. (2012). Changes in temporomandibular joint and ramus after sagittal split ramus osteotomy in mandibular prognathism patients with and without asymmetry. *Journal of Cranio-Maxillofacial Surgery*, 40(8), 821–827.

Yang, X.-W., Long, X., Yeweng, S.-J., and Kao, C.-T. (2007). Evaluation of mandibular setback after bilateral sagittal split osteotomy with the Hunsuck modification and miniplate fixation. *Journal of Oral and Maxillofacial Surgery*, 65(11), 2176–2180.